JACS
JOURNAL OF THE AMERICAN CHEMICAL SOCIETY
Article
pubs.acs.org/JACS

Structure-Based Design of a Potent Artificial Transactivation Domain Based on p53

Chantal Langlois,[†] Annarita Del Gatto,[‡] Geneviève Arseneault,[†] Julien Lafrance-Vanasse,[†] Mariarosaria De Simone,[‡] Thomas Morse,[†] Ivan de Paola,[‡] Mathieu Lussier-Price,[†] Pascale Legault,[†] Carlo Pedone,[‡] Laura Zaccaro,*[,‡] and James G. Omichinski*[,†]

[†]Département de Biochimie, Université de Montréal, C.P. 6128 Succursale, Centre-Ville, Montréal, Quebec H3C 3J7, Canada

[‡]Institute of Biostructures and Bioimaging, CNR and Department of Biological Sciences, University of Naples "Federico II", via Mezzocannone 16, 80134 Napoli, Italy

Supporting Information

ABSTRACT: Malfunctions in transcriptional regulation are associated with a number of critical human diseases. As a result, there is considerable interest in designing artificial transcription activators (ATAs) that specifically control genes linked to human diseases. Like native transcriptional activator proteins, an ATA must minimally contain a DNA-binding domain (DBD) and a transactivation domain (TAD) and, although there are several reliable methods for designing artificial DBDs, designing artificial TADs has proven difficult. In this manuscript, we present a structure-based strategy for designing short peptides containing natural amino acids that function as artificial TADs. Using a segment of the TAD of p53 as the scaffolding, modifications are introduced to increase the helical propensity of the peptides. The most active artificial TAD, termed E-Cap-(LL), is a 13-mer peptide that contains four key residues from p53, an N-capping motif and a dileucine hydrophobic bridge. In vitro analysis demonstrates that E-Cap-(LL) interacts with several known p53 target proteins, while in vivo studies in a yeast model system show that it is a 20-fold more potent transcriptional activator than the native p53-13 peptide. These results demonstrate that structure-based design represents a promising approach for developing artificial TADs that can be combined with artificial DBDs to create potent and specific ATAs.

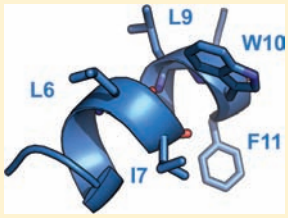

INTRODUCTION

Activation of transcription is regulated by a complex network of macromolecular interactions that leads to enhanced rates of gene expression, and one of the key components of this network are transcriptional activators.[1] Transcriptional activators are proteins minimally composed of a DNA-binding domain (DBD) and a transcription activation domain (TAD), and these two domains can exist either within the same protein or be assembled through protein−protein interactions.[1−3] The DBD functions to direct the activator to specific sites on DNA, whereas the TAD participates in several protein−protein interactions with multiple components of the transcriptional machinery, including nucleosome-remodeling complexes, histone acetyl transferases (HATs), and general transcription factors (TFIIB, TBP, TFIIH).[4−12]

Malfunctions in transcriptional regulation are associated with many human diseases and there is considerable interest in developing artificial transcription factors (ATFs) that can either activate or repress a specific gene.[13−18] Given the recent success using RNAi to repress expression of specific genes,[19−21] most current efforts are now focused in developing artificial transcriptional activators (ATAs). Like their natural counterparts, ATAs must minimally contain a DBD and a TAD. The design of artificial DBDs has benefited from the wealth of structural information available for DNA and protein:DNA complexes. The most successful examples of artificial DBDs include pyrole−imidazole polyamides (PIP),[22−24] peptide nucleic acids (PNA),[25−28] and engineered zinc-finger proteins.[29−31] In contrast to artificial DBDs, designing artificial TADs in an efficient and predictable manner has proven difficult.[13] Efforts to design artificial TADs are hampered by the fact that TADs interact with multiple target proteins as part of their normal function[4−12] and that there are only a limited number of high-resolution structures of TADs in complex with their target proteins. Structural studies of TADs are limited by the fact that most native TADs are intrinsically unstructured domains that must transition from a disordered to an ordered state to bind their targets.[32−38] This intrinsic flexibility has made it more difficult to crystallize TADs in complexes, and this has severely limited the available structural information.

The most practical solution in designing ATAs has been to attach the sequence from a native TAD to the artificial DBD of choice.[26,39−42] However, native TADs vary tremendously in size and complexity (ranging from 14 to 300+ amino acids) and often generate variable responses when incorporated into ATAs. Attempts to design shorter artificial TADs have generally started either by concatenating short sections from native TADs[14,41,43−46] or by screening peptide/peptoid libraries.[44,45,47−50] Unfortunately, these methods are limited by

Received: September 24, 2011
Published: December 19, 2011

   dx.doi.org/10.1021/ja208999e | J. Am. Chem.Soc. 2012, 134, 1715−1723

the fact that it is difficult to improve their design in a systematic manner in the absence of structural information. In addition, attempts to synthetically prepare small molecules that function as artificial TADs have proven to be very challenging.[44,51−53] This is also due to the shortage of structural information and the fact that TADs often bind over a large surface area when in complex with their partners, making it difficult to define a scaffold from which to base the design.

The herpes viral protein 16 (VP16) and the human tumor suppressor protein, p53, are two of the most potent transcriptional activator proteins known, and their TADs share several common features.[54−56] This includes being very acidic, containing two subdomains (p53TAD1/p53TAD2 and VP16N/VP16C), and interacting with many of the same target proteins.[54,55,57] We have previously determined the structures of the second subdomains from the TADs of p53 (p53TAD2) and VP16 (VP16C) in complex with the Tfb1 subunit of the general transcription factor IIH (TFIIH).[32,33] These structures demonstrated that p53TAD2 and VP16C both transition from an unstructured state to form a nine-residue amphipathic α-helix in complex with the pleckstrin homology domain of Tfb1 (Tfb1PH). Comparison of the two structures showed that three hydrophobic residues and one acidic residue located at positions four, five, seven, and eight in the helices of p53 (residues Ile50, Glu51, Trp53, and Phe54) and VP16 (residues Phe475, Glu476, Met478, Phe479) are crucial to formation of the interface with Tfb1PH. Although the three hydrophobic residues are not strictly conserved between p53 and VP16, they form similar interactions with Tfb1PH, and this suggests that either of these two structures could serve as a general template for the structure-based design of artificial TADs.

In this contribution, we report the design of an artificial TAD [E-Cap-(LL)] based on the structure TAD of p53 in complex with Tfb1PH. E-Cap-(LL) is a 13-residue peptide composed of natural amino acids, which preserves the four key residues of p53 that form the interface with Tfb1PH. In addition, E-Cap-(LL) contains an N-terminal capping motif (N-Cap) and two leucines spaced in an *i*, *i*+3 manner to increase its helical propensity. In vitro studies indicate that E-Cap-(LL) functions like p53TAD2 in a number of binding and competition assays. In addition, E-Cap-(LL) is an extremely potent in vivo transcriptional activator in yeast. E-Cap-(LL) is the first artificial TAD designed based on a known structure of a TAD bound to its target, and its potent in vivo activity indicates that structure-based design represents a promising approach for developing artificial TADs to be used in ATAs.

EXPERIMENTAL PROCEDURES

Chemical Peptide Synthesis and Purification. The p53-13, NC15, NC17, A-Cap-(LL), E-Cap-(LL), W-Cap-(LL), E-Cap-(DL), and E-Cap-(LQ) peptides were synthesized on solid phase and purified by HPLC (For further details see Supplementary Experimental Procedures in Supporting Information [SI]). The identity and purity of the peptides were verified by LC/MS spectrometry.

Cloning of Recombinant Proteins for Purification. The bacterial expressed p53 peptide analogues [E-Cap-(LL), p53-13, E-Cap-(DL), E-Cap-(LQ), and mutants] were constructed by inserting the *Bam*HI-EcoR1-digested DNA (IDT) into pGEX-2T plasmid. Tfb1PH was cloned as previously described.[32] Mutants of Tfb1PH, E-Cap-(LL), and p53-13-(LL) were prepared using the QuickChange II site-directed mutagenesis kit (Stratagene).

Protein Expression and Purification. The p53 peptide analogues and Tfb1PH, were expressed as GST-fusion proteins in *Escherichia coli* host strain TOPP2 and bound to GSH-resin (GE Healthcare) as previously described.[32] The resin bound protein was incubated overnight with thrombin (Calbiochem). After cleavage, the supernatant was purified by FPLC over a Q-Sepharose (p53 analogues) or a SP-Sepharose (Tfb1PH) high performance column. Uniformly (>98%) ^{15}N-labeled and ^{15}N-/^{13}C-labeled proteins were prepared in minimal media containing $^{15}NH_4Cl$ with or without $^{13}C_6$-glucose as the sole nitrogen and carbon source. The CBP KIX domain (provided by Alanna Schepartz, Yale University, New Haven, CT) was expressed as His-Tag fusion protein in *E. coli* host strain BL21 (DE3) and purified to homogeneity (See Supplementary Experimental Procedures, SI for details).

Circular Dichroism Studies. Circular dichroism (CD) studies were performed with synthetic peptides on a Jasco J-810 spectropolarimeter at 25 °C in 10 mM sodium phosphate (pH = 7.1). All peptide concentrations were determined by A_{280}. The results are reported as mean residue molar ellipticity [θ]. The intensities of [θ] at 215, 207, 190 nm, the cross over, and the $\theta_{222}/\theta_{207}$ ratio are reported for all peptides (Supplementary Table 1, SI).

Isothermal Titration Calorimetry (ITC) Studies. The ITC experiments were performed as previously described,[32] in 20 mM Tris (pH = 7.5) for Tfb1PH, or in 20 mM sodium phosphate (pH = 6.5) for the CBP KIX domain. For binding studies to wild-type Tfb1PH, synthetic peptides were used and these peptides were acetylated on the N-terminus and amidated on the C-terminus. For binding studies with the Tfb1PH mutants and the Kix domain of CBP, bacterial expressed peptides were used. The bacterial expressed proteins have a free amino group on the N-terminus and a free carboxyl group on the C-terminus. The protein concentrations were determined from A_{280}. All titrations were done at least in duplicates and were fit to a single binding site mechanism with 1:1 stoichiometry.

Media, Plasmids and Strains. All yeast strains were grown in synthetic complete media (SC; 0,67% yeast nitrogen base w/o amino acids, 2% glucose, and amino acids drop-out mix) lacking uracil and histidine. The EGY48 (Mat alpha leu2-3 his3-11,15 trp1-1 ura3-1 6lexAops-LEU2) strain was transformed with the LexA operator-Lac-Z fusion plasmid pSH18-34 combined with either pEG202NLS (pEG202 derivative with SV40 nuclear localization sequence between LexA and polylinker) as a negative control, pSH17-4 (GAL4-activation domain cloned into pEG202 backbone) as a positive control or pEG202NLS with LexA fused to the activation domains to be tested.[58]

ß-Galactosidase Activation Assay. Liquid ß-galactosidase assays were performed as previously described.[58] Results are presented as the mean of the percentages of the ß-galactosidase units of the tested peptides on the ß-galactosidase units of the GAL4 positive control ± standard error of the mean (SEM). Western blot analysis was performed with an anti-LexA antibody to verify expression of all LexA-fused peptides.

NMR Samples. For the NMR chemical shift mapping studies with labeled Tfb1PH, the samples consisted of 0.5 mM ^{15}N-Tfb1PH in 20 mM sodium phophate (pH = 6.5), 1 mM EDTA and 90% H_2O/10% D_2O; unlabeled p53 analogues [NC17, NC15, E-Cap-(LL), W-Cap-(LL), or A-Cap-(LL)] were added to a final ratio of 1:2. For the chemical shift mapping studies with labeled E-Cap-(LL) peptide, the sample consisted of 0.5 mM of ^{15}N-E-Cap-(LL) in 20 mM sodium phosphate (pH = 6.5), 1 mM EDTA and 90% H_2O/10% D_2O to which unlabeled Tfb1PH was added to a final ratio of 1:2. For the competition experiment, an HSQC was first collected with a sample containing 0.8 mM of ^{15}N-p53$_{40-73}$ (p53TAD2) in 20 mM sodium phosphate (pH = 6.5), 1.0 mM EDTA and 90% H_2O/10% D_2O. Then 1 mM of unlabeled Tfb1PH was added, and a second HSQC was collected. Finally, 0.8 mM of unlabeled E-Cap-(LL) peptide was added, and a third HSQC spectrum was recorded. The structural studies of the E-Cap-(LL) peptide in complex with Tfb1PH were performed on two samples. The first contained 0.5 mM of ^{15}N-E-Cap-(LL) and 0.5 mM unlabeled Tfb1PH in 20 mM sodium phosphate (pH = 6.5), 1 mM EDTA, and 90% H_2O/10% D_2O. The second sample contained 0.5 mM ^{15}N/^{13}C-Tfb1PH and 0.5 mM unlabeled E-Cap-(LL) in 20 mM sodium phosphate (pH = 6.5), 1 mM EDTA. For studies in D_2O, the sample was dissolved in 99.996% D_2O.

NMR Spectroscopy Experiments. The NMR experiments were carried out at 295 K on Varian Unity Inova 500, 600, and 800 MHz spectrometers. For the chemical shift mapping studies, two-dimensional (2D) $^{1}H/^{15}N$ HSQC were recorded. Intramolecular nuclear Overhauser effects (NOEs) for E-Cap-(LL) were obtained from 3D ^{15}N-edited NOESY-HSQC (τ_m = 140 ms)[59] and 2D $^{13}C/^{15}N$-{F1/F2}-filtered $^{1}H/^{1}H$ NOESY (τ_m = 40 and 100 ms).[60] The NMR data were processed with NMRPipe/NMRDraw[61] and analyzed with CcpNMR.[62]

Structures Calculations. The NOE-derived distance restraints were divided into four classes defined as strong (1.8−2.8 Å), medium (1.8−3.4 Å), weak (1.8−5.0 Å), and very weak (3.3−6.0 Å). Backbone dihedral angles were derived with the program TALOS.[63] The structures of E-Cap-(LL) were calculated using the program CNS,[64] with a combination of torsion angle and Cartesian dynamics[65] and starting from an extended structure with standard geometry. The quality of structures was assessed using PROCHEK-NMR.[66] The figures were generated with the program PyMol (http://www.pymol.org).

RESULTS AND DISCUSSION

p53TAD Analogues with an N-Cap and a C-Cap Motif. On the basis of the NMR structure of the p53TAD2/Tfb1PH complex,[32] we set out to design short peptide analogues that mimic both the in vitro binding properties and the in vivo activity of p53TAD2. We hypothesize that peptide analogues with increased helical propensity which retain four key residues (IEXWF) in the α-helix of p53TAD2 (residues 47 to 55 in p53) will mimic p53TAD2 and be stronger in vivo activators. In the first approach, capping motifs are introduced both at the N- and C-termini (N-Cap and C-Cap) of the four key residues in two peptides (NC17 and NC15) (Figure 1A). NC17 consists

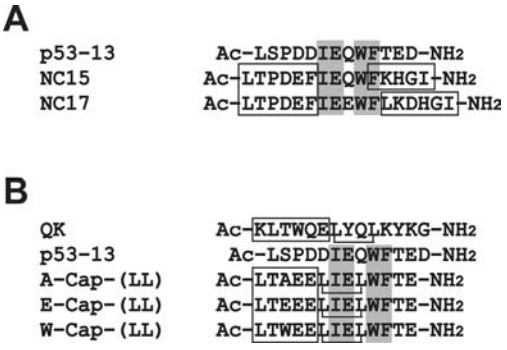

Figure 1. First and second designs of the p53TAD2 mimetics. (A) Sequence alignments of p53-13 with the NC15 and the NC17 peptides. The four key residues (IExWF) of the helical binding interface of p53TAD2/Tfb1PH complex are highlighted in gray. The residues included in N- and C-capping motifs are boxed. (B) Sequence alignments of p53-13 peptide with the VEGF helical analogue (QK), A-Cap-(LL), E-Cap-(LL) and W-Cap-(LL). As above, the key residues (IExWF) of the helical binding interface of p53TAD2/Tfb1PH complex are highlighted in gray and the N-capping motif is boxed. The two leucine residues forming the bridge with an *i*, *i*+3 spacing are shown connected by a bridge.

of 17 residues with an N-Cap and a C-Cap Schellman motif, which were chosen on the basis of statistical preference.[67,68] In NC17, the native Gln at position 51 is replaced by a Glu to favor stabilization of an *i*, *i*+4 salt bridge with the Lys in the C-Cap. NC15 is a 15-residue peptide, which contains the same N-Cap, but its C-Cap Schellman motif includes Trp53 and Phe54 from the native p53 sequence. NC15 and NC17 were prepared by solid phase peptide synthesis, and their helical character and affinity for Tfb1PH were analyzed using circular dichroism (CD) and isothermal titration calorimetry (ITC), respectively. The CD spectra demonstrate a significant increase in helical character for both NC15 and NC17 ($\theta_{222}/\theta_{207}$ ratio of 0.73 and 0.59, respectively) in comparison to p53-13 ($\theta_{222}/\theta_{207}$ ratio of 0.23), a control peptide corresponding to residues 45−57 of the TAD of p53 (Supplementary Table S1, SI). However, ITC experiments indicate that neither NC15 nor NC17 are able to bind Tfb1PH under the conditions tested (Figure 2A,B). The absence of binding by ITC is further supported by the lack of significant changes in chemical shifts during NMR titration experiments with Tfb1PH (data not shown). In comparison, we measure an apparent dissociation constant (K_d) of 1.6 ± 0.3 μM for the interaction of p53-13 with Tfb1PH under identical conditions (Figure 2B). Thus, although the addition of an N-Cap and a C-Cap increases the helical propensity, both NC15 and NC17 possess significantly lower affinity for Tfb1PH.

p53TAD Analogues with an N-Cap and a Leucine Bridge. In the second approach, we combined an N-cap with a hydrophobic bridge involving side chains from two leucine residues [(N-Cap-(LL) peptides] (Figure 1B). This approach is similar to the one used to develop the VEGF mimetic peptide QK (Figure 1B).[67,69] Three different N-Caps were tested and the resulting peptides are referred to as the A-Cap-(LL), E-Cap-(LL) and W-Cap-(LL) (LTAE, LTEE and LTWE N-Capping residues respectively). The E-Cap-(LL) motif was selected based on statistical probability,[68] the W-Cap-(LL) was chosen on the basis of the homology with the QK-peptide[67,69] and the A-Cap-(LL) was chosen on the basis of the homology with the N-Cap from the helix formed by VP16C.[33] The leucines were inserted with an *i*, *i*+3 spacing at positions 6 and 9 so that the hydrophobic interaction would form in the center of the peptide, but on the opposite face of the α-helix relative to the Tfb1PH binding interface (Figure 1B). The three peptides are all 13-residues long, and CD spectra recorded on the N-Cap-(LL) peptides indicate that they all possess approximately the same helical character [$\theta_{222}/\theta_{207}$ ratios of 0.52, 0.54, and 0.52 for A-Cap-(LL), E-Cap-(LL), and W-Cap-(LL) respectively], which is significantly higher than the p53-13 peptide (Supplementary Table S1, SI). Next, we measured the K_d values of the three peptides for Tfb1PH by ITC. The A-Cap-(LL) and W-Cap-(LL) have apparent K_d values of 1.3 ± 0.1 μM and 1.9 ± 0.3 μM, respectively, which is similar to that of p53-13 (K_d of 1.6 ± 0.3 μM), whereas the E-Cap-(LL) peptide has an apparent K_d of 0.19 ± 0.03 μM (Figure 2B). Thus, the introduction of a N-Cap in combination with a dileucine bridge improves the helical character of all three peptides and the E-Cap-(LL) peptide binds Tfb1PH with the highest affinity.

N-Cap-(LL) Analogues and p53TAD2 Share a Common Binding Site on Tfb1PH. To determine the binding site on Tfb1PH for the N-Cap-(LL) peptides, we performed NMR titration and displacement experiments. Addition of unlabeled E-Cap-(LL) to ^{15}N-labeled Tfb1PH produces changes in both the ^{1}H and ^{15}N chemical shifts for several signals in the $^{1}H/^{15}N$-HSQC spectrum of Tfb1PH (Supplementary Figure 1 A,B, SI). Like p53TAD2,[32] the residues that exhibited the most significant changes are located within the strands β5, β6, and β7 and in the loop between β5 and β6 when mapped on the structure of Tfb1PH (Figure 3A,B). Similar changes in chemical shifts are also observed in titrations of Tfb1PH with both A-Cap-(LL) (Supplementary Figure 1C, SI) and W-Cap-(LL) (Supplementary Figure 1D, SI). In addition, NMR displace-

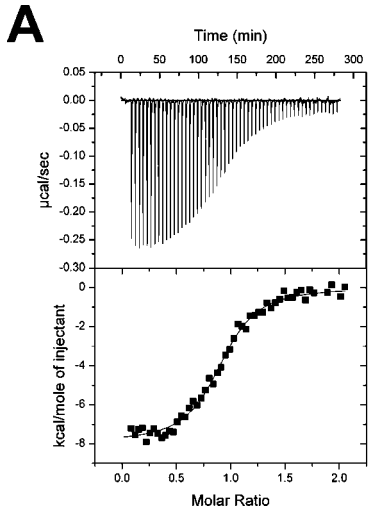

B

K_d values for Tfb1PH	
p53-13	1.6 ± 0.3 µM
NC15	NB
NC17	NB
A-Cap-(LL)	1.3 ± 0.1 µM
W-Cap-(LL)	1.9 ± 0.3 µM
E-Cap-(LL)	0.19 ± 0.03 µM

NB- K_d > 100 µM

Figure 2. Dissociation constants (K_d) for the interaction between Tfb1PH and the p53TAD2 analogues. (A) Representative ITC thermogram obtained by successive additions of synthetic E-Cap-(LL) into a solution of Tfb1PH. (B) Dissociation constants (K_d) for the binding of synthetic p53TAD2 peptide analogues to Tfb1PH as determined by ITC. All titrations fit the single binding site mechanism with 1:1 stoichiometry.

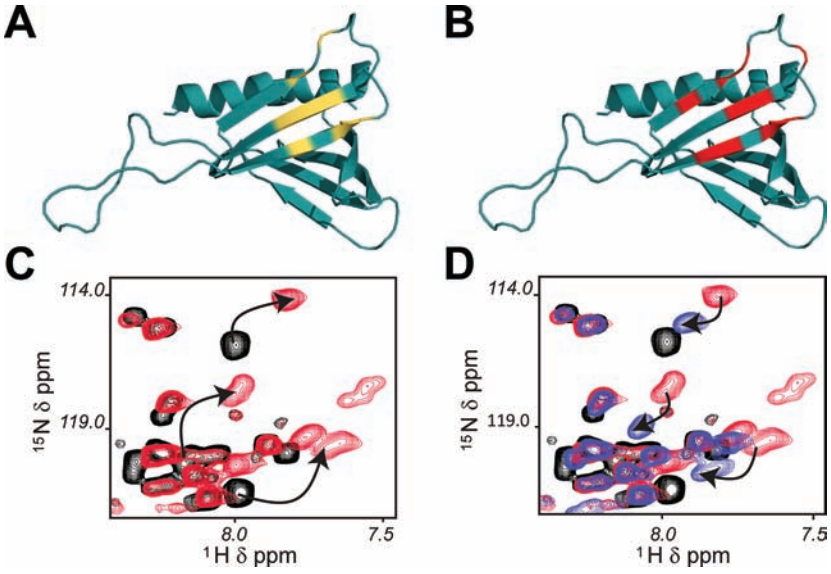

Figure 3. E-Cap-(LL) peptide share a common binding site on Tfb1PH with p53TAD2. (A,B) Ribbon model of the NMR structure of free Tfb1PH.[32] Residues that undergo significant chemical shift changes in the ^{1}H/^{15}N HSQC spectra of Tfb1PH upon formation of the Tfb1PH/p53TAD2 complex are mapped in yellow (A), or upon formation of the Tfb1PH/E-Cap-(LL) complex are mapped in red (B). (C) Overlay of a selected region from the two-dimensional ^{1}H/^{15}N HSQC spectra for a 0.8 mM sample of ^{15}N-labeled p53TAD2 in the free form (black) and in the presence of 1.0 mM unlabeled Tfb1PH (red). (D) Overlay of a selected region from the two-dimensional ^{1}H/^{15}N HSQC spectra for a 0.8 mM sample of ^{15}N-labeled p53TAD2 in the free form (black), in the presence of 1.0 mM unlabeled Tfb1PH (red), and after addition of 0.8 mM unlabeled E-Cap-(LL) peptide (blue). Signals of ^{15}N-labeled p53TAD2 that undergo significant changes in ^{1}H- and ^{15}N-chemical shifts upon formation of the complex with Tfb1PH, (C) and that return toward their original position following the addition of E-Cap-(LL) peptide (D) are indicated by arrows. See Supplementary Figure 1 in SI for spectra of titration of Tfb1PH with E-Cap-(LL), A-Cap-(LL) and W-Cap-(LL).

ment experiments demonstrate that p53TAD2 and E-Cap-(LL) (Figure 3C,D) compete for a common binding site on Tfb1PH.

In a previous study,[32] we identified five mutants of Tfb1PH [Tfb1PH (Q49A), Tfb1PH (K57E), Tfb1PH (M59A), Tfb1PH (R61E), and Tfb1PH (M88A)] that significantly perturb binding to p53TAD2. The five-point mutations are located on the surface of Tfb1PH within the β5, β6, and β7 strands (Figure 4A) and do not alter the structure of Tfb1PH. By ITC, we are unable to detect binding of E-Cap-(LL) to the R61A mutant ($K_d \geq 100$ μM) using this assay (Figure 4B). In addition, the Q49A and M88A mutants decrease the binding of Tfb1PH to E-Cap-(LL) by over 20-fold (K_d = 2.4 ± 0.2 μM and 1.9 ± 0.2 μM, respectively), whereas the K57E and the M59A mutants decrease binding by approximately 10-fold (K_d = 1.0 ± 0.1 μM and 0.9 ± 0.09 μM, respectively). These results support that E-Cap-(LL) is forming very similar interactions with Tfb1PH as seen with p53TAD2.

E-Cap-(LL) binds to CBP/p300. CREB-binding protein (CBP) and p300 (CBP/p300) are two highly homologous HATs that have been shown to play an important role in regulating a number of transcriptional activators including p53.[70,71] Four domains of CBP/p300 (TAZ1/CH1, TAZ2/CH3, KIX, and IBiD) have been shown to interact with the TAD of p53, and acetylation of p53 by CBP/p300 is essential

dx.doi.org/10.1021/ja208999e | J. Am. Chem.Soc. 2012, 134, 1715−1723

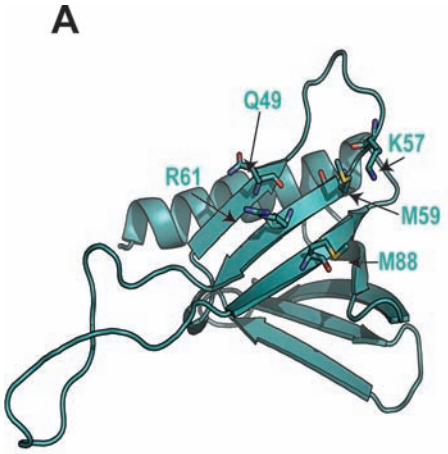

B K_d values of E-Cap-(LL) for Tfb1PH mutants

Tfb1PH WT	0.09 ± 0.01 μM
Tfb1PH (Q49A)	2.4 ± 0.2 μM
Tfb1PH (K57E)	1.0 ± 0.1 μM
Tfb1PH (M59A)	0.9 ± 0.1 μM
Tfb1PH (R61A)	NB
Tfb1PH (M88A)	1.9 ± 0.2 μM

NB- K_d > 100 μM

C K_d values of E-Cap-(LL) for CBP/p300 domains

CBP KIX	3.8 ± 0.8 μM
CBP IBiD	0.9 ± 0.1 μM

Figure 4. Comparison of the dissociation constants (K_d) of E-Cap-(LL) binding to p53 target proteins. (A) Ribbon model of the NMR structure of Tfb1PH. The five residues located on the surface of Tfb1PH within the β5, β6, and β7 strands that are mutated are highlighted. (B) Comparison of the dissociation constants (K_d) for the interaction of the bacterial expressed E-Cap-(LL) analogue with Tfb1PH and the five mutants as determined by ITC measurements. (C) Comparison of the dissociation constants (K_d) for the interaction of the bacterial expressed E-Cap-(LL) analogue with the KIX and IBiD domains of CBP/p300 as determined by ITC measurements.

for p53-dependent activation.[72,73] ITC studies demonstrate that E-Cap-(LL) is able to interact with both the KIX and IBiD domains of CBP/p300 (K_d = 3.8 ± 0.8 μM and 0.84 ± 0.12 μM, respectively; Figure 4C). These results indicate that, like the TAD of p53, E-Cap-(LL) is able to interact with domains of CBP/p300.

E-Cap-(LL) Is a Potent Activator in Vivo. To verify that E-Cap-(LL) activates transcription in vivo, it was fused to the DNA-binding domain (DBD) of LexA, and its activation potential was measured in yeast cells. The activity of E-Cap-(LL) for the *lacZ* reporter gene is measured relative to a positive control (Gal4 TAD-LexA-DBD) whose activity is established as 100%. In this system, the E-Cap-(LL)-LexA-DBD fusion protein activates transcription at 161 ± 9% of the positive control. In comparison, the native p53-13 peptide fused to the LexA-DBD activates transcription at only 8 ± 3%. Thus, E-Cap-(LL) is ~20 times more potent than p53-13 as a transcriptional activator in this in vivo system (Figure 5). To compare the in vivo activity of the E-Cap-(LL) relative to other known artificial TADs, we compared its activity relative to two model artificial TADs, the AH[47] and VP2[45] peptides. The AH-LexA-DBD and VP2-LexA-DBD activate transcription at approximately 5% of the positive control (Figure 5) which is similar to p53-13, but over 30-fold less than E-Cap-(LL) .These results strongly support the idea that stabilizing the helical character of short analogues of p53TAD2 can lead to a significant enhancement of their in vivo transcriptional activity.

The Role of Leucines for the in Vivo Activity of the p53TAD Analogues. To investigate the role that the two leucine residues play in the ability of E-Cap-(LL) to activate transcription in vivo, we mutated the leucine residue at position 9 to the native glutamine residue found in p53-13 to generate E-Cap-(LQ). This change lowers the in vivo activity to 67 ± 8% of the positive control, and thus E-Cap-(LQ) is ~50% less active than E-Cap-(LL) (161 ± 9%; Figure 5). Next, we inserted two leucine residues at equivalent positions of p53-13 to generate p53-13-(LL). The in vivo transcriptional activation of p53-13-(LL) is 10-fold higher than that of p53-13 (95 ± 6% versus 8 ± 3%), but 50% less active than that of E-Cap-(LL) (Figure 5). These results support the idea that both the N-Cap

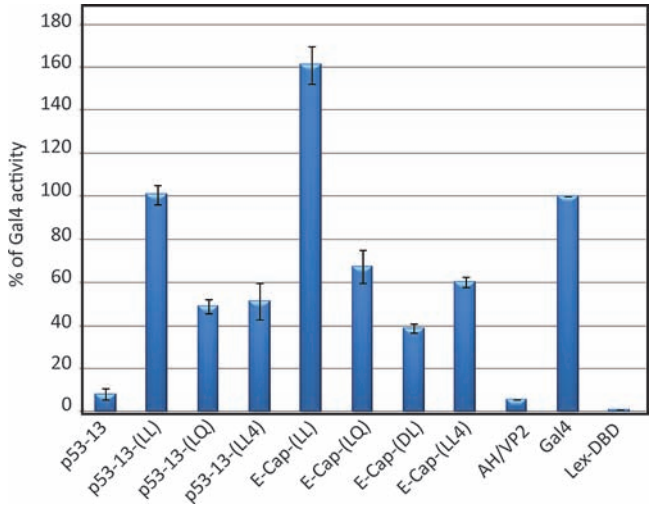

Figure 5. E-Cap-(LL) functions as a potent activation domain in yeast. LexA-peptide fusion proteins were cotransformed into yeast with the reporter LexA operator-Lac-Z fusion plasmid pSH18-34. Results are presented as the mean of the percentages of the β-galactosidase units of the tested fusion proteins on the β-galactosidase units of the LexA-GAL4TAD positive control. Error bars represent standard error about the mean of a minimum of three independent experiments.

motif, and the dileucine-bridge contribute significantly to the in vivo transcriptional activity of E-Cap-(LL).

Peptides with Leucines in the *i*, *i*+4 Spacing Are Less Active in Vivo. Experimental and theoretical studies indicate that two hydrophobic amino acids separated by either three (*i*, *i*+3 spacing pattern) or four residues (*i*, *i*+4 spacing pattern) enhance the helical propensity of peptides through side-chain interactions.[74−78] Given that the insertion of the two leucines with an *i*, *i*, *i*+3 spacing pattern enhances the in vivo activation of E-Cap-(LL) and p53-13-(LL), we tested the role of leucines with an *i*, *i*+4 spacing pattern on in vivo activity. Leucine residues were introduced at positions 4 and 8 in the p53-13 peptide [p53-13-(LL4)] and at positions 5 and 9 in the E-Cap-(LL) peptide [E-Cap-(LL4)] (Figure 5). These positions are again chosen in an attempt to place the leucine bridge in the center of the peptide, but on the backside of the helix relative to

dx.doi.org/10.1021/ja208999e | J. Am. Chem.Soc. 2012, 134, 1715−1723

the Tfb1PH binding interface. In the yeast activation assay, LexA-p53-13-(LL4) displays 51 ± 8% of the activity of GAL4-LexA (Figure 5). This corresponds to a 6−7-fold increase in activity compared to that of the native p53-13 (8 ± 3%), but only about half of the activity that we observe when the leucines are in the *i*, *i*+3 spacing pattern in p53-13-(LL) (95 ± 6%). Similarly, E-Cap-(LL4) displays 60 ± 2% of the activity of GAL4-LexA, but this corresponds to roughly 40% of the activity compared to E-Cap-(LL) (161 ± 9%). The increased in vivo activity observed when two leucines were inserted in either the *i*, *i*+3 or *i*, *i*+4 spacing pattern of p53-13 is consistent with in vitro studies with model peptides showing that both spacing patterns are able to increase their helical propensity/stability.[74−78]

E-Cap-(LL) Forms a Helix in Complex with Tfb1PH. We have previously shown that p53TAD2 transitions from an unstructured state to form a nine-residue α-helix upon binding to Tfb1PH.[32] In this work, we attempted to increase the helical propensity of the same region of p53TAD2 by adding an N-Cap and a dileucine bridge. Although CD studies indicate that E-Cap-(LL) possesses a higher helical content than p53-13 (Supplementary Table 1, SI), NMR experiments with E-Cap-(LL) did not show the presence of NOE signals characteristic of an α-helical conformation in the free form (Supplementary Figure 2, SI). Additional NMR studies of E-Cap-(LL) in complex with Tfb1PH show that, like p53TAD2, it transitions to form a nine-residue α-helix from Glu3 to Phe11 (Figure 6A,B and Supplementary Figure 2, SI). The structure of the E-Cap-(LL) peptide in complex with Tfb1PH is calculated from 105 NOE-derived distance restraints and 22 dihedral angle restraints. An analysis of the 20 lowest-energy structures indicates that they have no NOE violation greater than 0.2 Å, no backbone dihedral angle violation greater than 2°, and low pairwise rmsd values (Table 1). The structure of E-Cap-(LL) in complex with Tfb1PH confirms that the side chains of Leu6 and Leu9 are in close proximity to each other and on the opposite side of the helix relative to the binding interface with Tfb1PH (Figure 6C,D). In addition, the side chain of Leu6 is in position to further stabilize the helix through contacts with the aromatic ring of Trp10 in the *i*+4 position (Figure 6E,F).

Both *i*, *i*+3 and *i*, *i*+4 side-chain interactions contribute to E-Cap-(LL) activity. The NMR studies clearly indicate that Leu6 in the E-Cap-(LL) peptide is in position to enhance the stability of the helix through both *i*, *i*+3 interactions (L6-L9) and *i*, *i*+4 interactions (L6-W10). In order to verify this observation, two additional mutants were tested. In p53-13-(LQ), the second leucine of p53-13-(LL) is replaced with the native glutamine residue, whereas in the E-Cap-(DL) the first leucine of E-Cap-(LL) is replaced with the native aspartic acid residue of p53. In the yeast activation assay, LexA-p53-13-(LQ) displays 45 ± 8% of the activity of the control (Figure 5). This corresponds to a 5-fold increase in activity compared to the p53-13 peptide (8 ± 3%), but less than half of the activity we observe when the leucines are in the *i*, *i*+3 spacing pattern in p53-13-(LL) (95 ± 6%). Likewise, E-Cap-(DL) displays 35 ± 4% of the activity of the GAL4-LexA positive control, and this corresponds to roughly one-half of the activity of the E-Cap-(LQ) (67 ± 8%). Consistent with the NMR structure of the E-Cap-(LL) peptide bound to Tfb1PH, these results indicate that both *i*, *i*+3 interactions (L6-L9) and *i*, *i*+4 interactions (L6-W10) are contributing to the in vivo activity of the p53-13-(LL) and E-Cap-(LL) analogues.

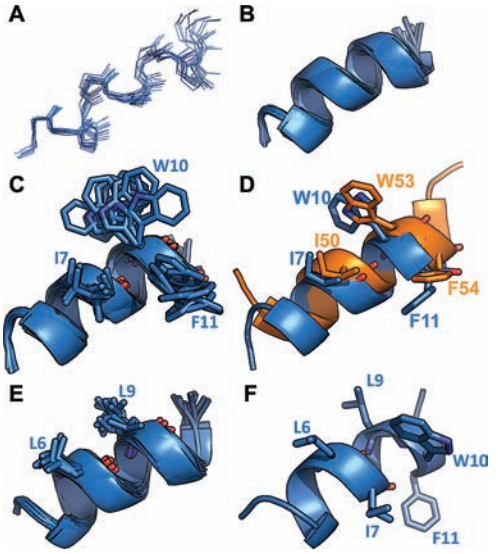

Figure 6. NMR structure of E-Cap-(LL) peptide in complex with Tfb1PH. (A) Overlay of the 10 lowest-energy structures of the E-Cap-(LL) peptide in complex with Tfb1PH. The structures were superimposed using the backbone atoms C′, C^{α}, and N. (B) Ribbon model of the 10 lowest-energy conformers of the E-Cap-(LL) peptide. (C) Overlay of the 10 lowest-energy conformers of the E-Cap-(LL) peptide showing the relative position of the three hydrophobic residues I7, W10, and F11. (D) Overlay of residues 45−57 of p53TAD2 (in orange) and the average structure of E-Cap-(LL) peptide (in blue). The three key hydrophobic residues I50, W53, and F54 of p53TAD2 are located in orientations similar to those of I7, W10, and F11 of the E-Cap-(LL) peptide. (E) Ribbon model of the 10 lowest-energy conformers of the E-Cap-(LL) peptide from the complex with Tfb1PH. The side chains of the leucines (L6 and L9) that form the bridge are highlighted. (F) Ribbon model of the average structure of the E-Cap-(LL) peptide from the complex with Tfb1PH. The side chains of the three hydrophobic residues (I7, W10, and F11) and the leucines (L6 and L9) are highlighted to show that they are on opposite faces of the helix. See Supplementary Figure 2 in SI for NMR spectra of E-Cap-(LL) in the absence and presence of Tfb1PH.

CD studies demonstrate that the E-Cap-(LQ) peptide ($\theta_{222}/\theta_{207}$ ratio of 0.41) has a higher helical propensity than the E-Cap-(DL) peptide ($\theta_{222}/\theta_{207}$ ratio of 0.25), and both have a lower helical propensity than the E-Cap-(LL) peptide ($\theta_{222}/\theta_{207}$ ratio of 0.54) peptides (Supplementary Table S1, SI). Furthermore, both the E-Cap-(LQ) and the E-Cap-(DL) peptides bind with slightly lower affinities to both Tfb1PH and the KIX domain of CBP/p300 in comparison to the E-Cap-(LL) peptide (Supplementary Table S2, SI). Thus, there is a good correlation between the transactivation activities of these peptides and both their helical propensity and binding affinities. However, given our results with the NC15 and NC17 peptides, neither one is sufficient by itself to predict the in vivo transactivation activity.

■ CONCLUSION

ATAs have enormous potential for use as either therapeutic agents for treating human diseases or as biological probes for investigating the correlation between aberrant transcription and human diseases.[13,14] In designing an ATA, the ultimate goal is to construct both the DBD and the TAD component as efficiently as possible while maintaining both specificity and activity.[13] There are now several methods for designing artificial DBDs that depend extensively on the availability of high-

Table 1. Structural Statistics for E-Cap-(LL) in Complex with Tfb1PH[a]

restraints used for the structure calculations	
total number of NOE distances restraints	105
short-range (intraresidue)	49
medium-range ($\|i-j\| \leq 4$)	56
long-range	0
number of dihedral angle restraints (φ, ψ)	22
structural statistics	
rms deviations from idealized geometry	
bonds (Å)	0.0027 ± 0.00007
angles (deg)	0.4025 ± 0.0038
impropers (deg)	0.231745 ± 0.0111
rms deviations from distance restraints (Å)	0.0240 ± 0.0005
rms deviations from dihedral restraints (deg)	1.1482 ± 0.015
Ramachandran statistics (%)[b]	
residues in most favored regions	69.2
residues in additional allowed regions	30.8
residues in generously allowed regions	0
residues in disallowed regions	0
coordinate precision[c]	
atomic pair wise rmsd (Å)	
E-Cap-(LL) in complex	
backbone atoms (C′, C^{α}, N)	0.50 ± 0.17
all heavy atoms	1.72 ± 0.32

[a]The 20 conformers with the lowest energies were selected for statistical analysis. [b]Based on PROCHECK-NMR analysis.

resolution structural information of protein:DNA complexes.[22,23,25−27,29] In contrast, there is far less structural information available for TADs in complex with their target proteins, and this is mostly due to the fact that TADs are generally intrinsically disordered in their free state. Unfortunately, this flexibility and adaptability adds to the complexity of designing artificial TADs. Thus, the key step for preparing a minimal artificial TAD is to identify structures of TADs in complex with target proteins that could serve as models for the design of artificial TADs.

In this work, we used the structure of the TAD of p53 bound to Tfb1PH as a template for designing ATAs.[32] Our hypothesis was that if we could enhance the helical propensity of the Tfb1PH interacting region from the TAD of p53 this would yield a more potent artificial TAD. Like p53, our designed peptide E-Cap-(LL) forms a nine-residue α-helix when in complex with Tfb1PH and binds along the same interface. The binding interface is a shallow groove surrounded by positively charged residues that help position the negatively charged TAD so that its hydrophobic residues can participate in a series of van der Waals contacts with hydrophobic pockets dispersed along the groove. Superposition of the hydrophobic residues from p53TAD2 and E-Cap-(LL) peptide when bound to Tfb1PH demonstrates that the residues from the IExWF motif [Ile6-Phe11 in E-Cap-(LL)] are located in virtually identical positions (Figure 6D), and E-Cap-(LL) appears to make the same contacts with Tfb1PH as p53TAD2. The structure is further supported by our ITC results in which mutations of the Tfb1PH residues (Gln49, Lys57, Met59, Arg61, and Met88) contributing to the interface with p53TAD2[32] also disrupt binding of the E-Cap-(LL) peptide (Figure 4A,B).

The increased in vivo potency of E-Cap-(LL) relative to the native p53-13 peptide appears to be directly linked to its enhanced helical stability since both the N-Cap motif and the two leucines are required for maximal activity. The introduction of the hydrophobic interaction on the face opposite to the Tfb1PH interacting interface represents a potentially valuable strategy in designing artificial TADs with increased in vivo activity. Previous experimental studies with model peptides suggested that hydrophobic amino acids with an *i*, *i*+4 spacing pattern had a slightly higher helix stabilizing effect than those with an *i*, *i* +3 spacing pattern, but that either pattern can significantly increase the helical propensity of peptides relative to alanine.[74−77] Likewise, Monte Carlo simulations predict that the *i*, *i*+3 and *i*, *i*+4 spacing of leucines can enhance helical stability, but differ from the experimental results by suggesting that *i*, *i*+3 spacing should be more effective.[78] In the case of the E-Cap-(LL) peptide, our mutation studies provide evidence that Leu6 can participate in *i*, *i*+3 interaction with Leu9 and *i*, *i* +4 interaction with Trp10, and thus, both types of interactions are functioning. The fact that the NMR studies of E-Cap-(LL) in complex demonstrate the presence of both the *i*, *i*+3 and the *i*, *i*+4 interactions further confirms the important role of these interactions for the in vitro binding and in vivo activity.

The importance of the spacing patterns for bridging interactions has also been observed with other helical stabilizing procedures such as stapled peptides and β-peptides.[79−81] It is clear that the location plays a huge factor when introducing helix-stabilizing modifications, and that structural characterization can aid tremendously in selecting the location. In the case of E-Cap-(LL), it must still undergo a transition from partially unstructured to the helical conformation that binds Tfb1PH. However, the activation energy required for this transition is lowered by the presence of the N-Cap and the leucines, and this ultimately leads to a significantly higher level of activity in vivo. The key question that still remains is whether we can design a peptide locked in a helical conformation that would further enhance the activity in vivo beyond what we observe with E-Cap-(LL). To function in vivo TADs must interact with multiple targets using a "flycasting"-like method,[82] and it may be crucial that, like E-Cap-(LL), they retain a minimal amount of flexibility to bind optimally to their different targets. Future studies are required to test this possibility using more constrained analogues of E-Cap-(LL) and structural studies will be crucial to developing and optimizing such constrained analogues.

■ ASSOCIATED CONTENT

Supporting Information

Supplementary procedures describe details of peptide synthesis and protein purification. Supplementary Table 1 shows the results of circular dichroism studies. Supplementary Table 2 shows binding results of the E-Cap-(LQ) and E-Cap-(DL) peptides with Tfb1PH and the Kix domain of CBP/p300. Supplementary Figure 1 shows HSQC spectra from NMR chemical shift perturbations studies of E-Cap-(LL) and A-Cap-(LL) with ^{15}N-labeled Tfb1PH. Supplementary Figure 2 shows HSQC spectra from NMR chemical shift perturbations studies of Tfb1PH with ^{15}N-labeled E-Cap-(LL). This information is available free of charge via the Internet at http://pubs.acs.org.

■ AUTHOR INFORMATION

Corresponding Author

jg.omichinski@umontreal.ca; lzaccaro@unina.it

■ ACKNOWLEDGMENTS

We thank Dr. G. Perretta and Mr. L. De Luca for technical assistance, and Drs. Paola Di Lello and Luca D'Andrea for helpful comments. We thank Alanna Schepartz for the CBP-Kix clone used in this work. This work was supported by grant 019360 from the Canadian Cancer Society (J.G.O.). C.L. is a recipient of a Postdoctoral Fellowship from the FRSQ. J.L-V. is a Vanier Canada Graduate Scholar from the CIHR. T.M. is the recipient of a graduate fellowship from the CIHR. P.L. is a recipient of a Canadian Research Chair in Structural Biology and Engineering of RNA.

■ REFERENCES

(1) Ptashne, M.; Gann, A. A. F. *Nature* **1997**, *386*, 569.
(2) Giniger, E.; Ptashne, M. *Nature* **1987**, *330*, 670.
(3) Sadowski, I.; Ma, J.; Triezenberg, S.; Ptashne, M. *Nature* **1988**, *335*, 563.
(4) Goodrich, J. A.; Hoey, T.; Thut, C. J.; Admon, A.; Tjian, R. *Cell* **1993**, *75*, 519.
(5) Brown, C. E.; Howe, L.; Sousa, K.; Alley, S. C.; Carrozza, M. J.; Tan, S.; Workman, J. L. *Science* **2001**, *292*, 2333.
(6) Prochasson, P.; Neely, K. E.; Hassan, A. H.; Li, B.; Workman, J. L. *Mol. Cell* **2003**, *12*, 983.
(7) Yang, F.; DeBeaumont, R.; Zhou, S.; Naar, A. M. *Proc. Natl. Acad. Sci. U.S.A.* **2004**, *101*, 2339.
(8) Blau, J.; Xiao, H.; McCracken, S.; O'Hare, P.; Greenblatt, J.; Bentley, D. *Mol. Cell. Biol.* **1996**, *16*, 2044.
(9) Tansey, W. P.; Ruppert, S.; Tjian, R.; Herr, W. *Genes Dev.* **1994**, *8*, 2756.
(10) Black, J. C.; Choi, J. E.; Lombardo, S. R.; Carey, M. *Mol. Cell* **2006**, *23*, 809.
(11) Gutierrez, J. L.; Chandy, M.; Carrozza, M. J.; Workman, J. L. *EMBO J.* **2007**, *26*, 730.
(12) Brown, S. A.; Weirich, C. S.; Newton, E. M.; Kingston, R. E. *EMBO J.* **1998**, *17*, 3146.
(13) Lee, L. W.; Mapp, A. K. *J. Biol. Chem.* **2010**, *285*, 11033.
(14) Graslund, T.; Li, X.; Magnenat, L.; Popkov, M.; Barbas, C. F. III. *J. Biol. Chem.* **2005**, *280*, 3707.
(15) Rodriguez-Martinez, J. A.; Peterson-Kaufman, K. J.; Ansari, A. Z. *Biochim. Biophys. Acta Gene Reg. Mech.* **2010**, *1799*, 768.
(16) Sera, T. *Adv. Drug Delivery Rev.* **2009**, *61*, 513.
(17) Visser, A. E.; Verschure, P. J.; Gommans, W. M.; Haisma, H. J.; Rots, M. G. *Adv. Genet.* **2006**, *56*, 131.
(18) Verschure, P. J.; Visser, A. E.; Rots, M. G. *Adv. Genet.* **2006**, *56*, 163.
(19) Hannon, G. J. *Nature* **2002**, *418*, 244.
(20) Rana, T. M. *Nat. Rev. Mol. Cell Biol.* **2007**, *8*, 23.
(21) Kim, D. H.; Rossi, J. J. *Nat. Rev. Genet.* **2007**, *8*, 173.
(22) Dervan, P. B.; Doss, R. M.; Marques, M. A. *Curr. Med. Chem. Anticancer Agents* **2005**, *5*, 373.
(23) Nickols, N. G.; Jacobs, C. S.; Farkas, M. E.; Dervan, P. B. *Nucleic Acids Res.* **2007**, *35*, 363.
(24) Muzikar, K. A.; Nickols, N. G.; Dervan, P. B. *Proc. Natl. Acad. Sci. U.S.A.* **2009**, *106*, 16598.
(25) Nielsen, P. E. *Q. Rev. Biophys.* **2005**, *38*, 345.
(26) Chen, J.; Peterson, K. R.; Iancu-Rubin, C.; Bieker, J. J. *Proc. Natl. Acad. Sci. U.S.A.* **2010**, *107*, 16846.
(27) Liu, B.; Han, Y.; Corey, D. R.; Kodadek, T. *J. Am. Chem. Soc.* **2002**, *124*, 1838.
(28) Nielsen, P. E.; Egholm, M.; Berg, R. H.; Buchardt, O. *Science* **1991**, *254*, 1497.
(29) Beerli, R. R.; Barbas, C. F. III. *Nat. Biotechnol.* **2002**, *20*, 135.
(30) Beerli, R. R.; Dreier, B.; Barbas, C. F. III. *Proc. Natl. Acad. Sci. U.S.A.* **2000**, *97*, 1495.
(31) Beerli, R. R.; Schopfer, U.; Dreier, B.; Barbas, C. F. III. *J. Biol. Chem.* **2000**, *275*, 32617.
(32) Di Lello, P.; Jenkins, L. M. M.; Jones, T. N.; Nguyen, B. D.; Hara, T.; Yamaguchi, H.; Dikeakos, J. D.; Appella, E.; Legault, P.; Omichinski, J. G. *Mol. Cell* **2006**, *22*, 731.
(33) Langlois, C.; Mas, C.; Di Lello, P.; Jenkins, L. M. M.; Legault, P.; Omichinski, J. G. *J. Am. Chem. Soc.* **2008**, *130*, 10596.
(34) Uesugi, M.; Nyanguile, O.; Lu, H.; Levine, A. J.; Verdine, G. L. *Science* **1997**, *277*, 1310.
(35) Radhakrishnan, I.; PerezAlvarado, G. C.; Parker, D.; Dyson, H. J.; Montminy, M. R.; Wright, P. E. *Cell* **1997**, *91*, 741.
(36) Dames, S. A.; Martinez-Yamount, M.; Guzman, R. N. D.; Dyson, H. J.; Wright, P. E. *Proc. Natl. Acad. Sci. U.S.A.* **2002**, *99*, 5271.
(37) Wojciak, J. M.; Martinez-Yamout, M. A.; Dyson, H. J.; Wright, P. E. *EMBO J.* **2009**, *28*, 948.
(38) Kussie, P. H.; Gorina, S.; Marechal, V.; Elenbaas, B.; Moreau, J.; Levine, A. J.; Pavletich, N. P. *Science* **1996**, *274*, 948.
(39) Mattei, E.; Corbi, N.; Di Certo, M. G.; Strimpakos, G.; Severini, C.; Onori, A.; Desantis, A.; Libri, V.; Buontempo, S.; Floridi, A.; Fanciulli, M.; Baban, D.; Davies, K. E.; Passananti, C. *PLoS One* **2007**, *2*, e774.
(40) Lu, Y.; Tian, C.; Danialou, G.; Gilbert, R.; Petrof, B. J.; Karpati, G.; Nalbantoglu, J. *J. Biol. Chem.* **2008**, *283*, 34720.
(41) Stanojevic, D.; Young, R. A. *Biochemistry* **2002**, *41*, 7209.
(42) Di Certo, M. G.; Corbi, N.; Strimpakos, G.; Onori, A.; Luvisetto, S.; Severini, C.; Guglielmotti, A.; Batassa, E. M.; Pisani, C.; Floridi, A.; Benassi, B.; Fanciulli, M.; Magrelli, A.; Mattei, E.; Passananti, C. *Hum. Mol. Genet.* **2010**, *19*, 752.
(43) Wilber, A.; Tschulena, U.; Hargrove, P. W.; Kim, Y. S.; Persons, D. A.; Barbas, C. F. III; Nienhuis, A. W. *Blood* **2010**, *115*, 3033.
(44) Rowe, S. P.; Casey, R. J.; Brennan, B. B.; Buhrlage, S. J.; Mapp, A. K. *J. Am. Chem. Soc.* **2007**, *129*, 10654.
(45) Ansari, A. Z.; Mapp, A. K.; Nguyen, D. H.; Dervan, P. B.; Ptashne, M. *Chem. Biol.* **2001**, *8*, 583.
(46) Beltran, A. S.; Sun, X.; Lizardi, P. M.; Blancafort, P. *Mol. Cancer Ther.* **2008**, *7*, 1080.
(47) Ma, J.; Ptashne, M. *Cell* **1987**, *51*, 113.
(48) Xiao, X.; Yu, P.; Lim, H. S.; Sikder, D.; Kodadek, T. *Angew. Chem., Int. Ed.* **2007**, *46*, 2865.
(49) Liu, B.; Alluri, P. G.; Yu, P.; Kodadek, T. *J. Am. Chem. Soc.* **2005**, *127*, 8254.
(50) Xiao, X.; Yu, P.; Lim, H. S.; Sikder, D.; Kodadek, T. *J. Comb. Chem.* **2007**, *9*, 592.
(51) Jung, D. J.; Shimogawa, H.; Kwon, Y.; Mao, Q.; Sato, S.; Kamisuki, S.; Kigoshi, H.; Uesugi, M. *J. Am. Chem. Soc.* **2009**, *131*, 4774.
(52) Jung, D. J.; Choi, Y. M.; Uesugi, M. *Drug Discovery Today* **2006**, *11*, 452.
(53) Minter, A. R.; Brennan, B. B.; Mapp, A. K. *J. Am. Chem. Soc.* **2004**, *126*, 10504.
(54) Candau, R.; Scolnick, D. M.; Darpino, P.; Ying, C. Y.; Halazonetis, T. D.; Berger, S. L. *Oncogene* **1997**, *12*, 807.
(55) Triezenberg, S. J.; Kingsbury, R. C.; McKnight, S. L. *Genes Dev.* **1988**, *2*, 718.
(56) Unger, T.; Nau, M. M.; Segal, S.; Minna, J. D. *EMBO J.* **1992**, *11*, 1383.
(57) Sullivan, S. M.; Horn, P. J.; Olson, V. A.; Koop, A. H.; Niu, W.; Ebright, R. H.; Triezenberg, S. J. *Nucleic Acid Res.* **1998**, *26*, 4487.
(58) Di Lello, P.; Jenkins, L. M. M.; Mas, C.; Langlois, C.; Malitskaya, E.; Fradet-Turcotte, A.; Archambault, J.; Legault, P.; Omichinski, J. G. *Proc. Natl. Acad. Sci. U.S.A.* **2008**, *105*, 106.
(59) Marion, D.; Kay., L. E.; Sparks, S. W.; Torchia., D. A.; Bax, A. *J. Am. Chem. Soc.* **1989**, *111*, 1515.
(60) Ikura, M.; Bax, A. *J. Am. Chem. Soc.* **1992**, *114*, 2433.
(61) Delaglio, F.; Grzesiek, S.; Vuister, G. W.; Zhu, G.; Pfeifer, J.; Bax, A. *J. Biomol. NMR* **1995**, *6*, 277.
(62) Vranken, W. F.; Boucher, W.; Stevens, T. J.; Fogh, R. H.; Pajon, A.; Llinas, P.; Ulrich, E. L.; Markley, J. L.; Ionides, J.; Laue, E. D. *Proteins* **2005**, *59*, 687.
(63) Cornilescu, G.; Delaglio, F.; Bax, A. *J. Biomol. NMR* **1999**, *13*, 289.

(64) Brunger, A. T.; Adams, P. D.; Clore, G. M.; Gros, P.; Grosse-Kunstleve, R. W.; Jiang, J.-S.; Kuszewski, J.; Nilges, M.; Pannu, N. S.; Read, R. J.; Rice, L. M.; Simonson, T.; Warren, G. L. *Acta Crystallogr.* **1998**, *D54*, 905.
(65) Choy, W.-Y.; Tollinger, M.; Mueller, G. A.; Kay, L. E. *J. Biomol. NMR* **2001**, *21*, 31.
(66) Laskowski, R. A.; Antoon, J.; Rullmann, C.; Macarthur, M. W.; Kaptein, R.; Thornton, J. M. *J. Biomol. NMR* **1996**, *8*, 477.
(67) D'Andrea, L. D.; Iaccarino, G.; Fattorusso, R.; Sorriento, D.; Carannante, C.; Capasso, D.; Trimarco, B.; Pedone, C. *Proc. Natl. Acad. Sci. U.S.A.* **2005**, *102*, 14215.
(68) Aurora, R.; Rose, G. D. *Protein Sci.* **1998**, *7*, 21.
(69) Diana, D.; Ziaco, B.; Colombo, G.; Scarabelli, G.; Romanelli, A.; Fedone, C.; Fattorusso, R.; D'Andrea, L. D. *Chem.—Eur. J.* **2008**, *14*, 4164.
(70) Gu, W.; Roeder, R. G. *Cell* **1997**, *90*, 595.
(71) Avantaggiati, M. L.; Ogryzko, V.; Gardner, K.; Giordano, A.; Levine, A. S.; Kelly, K. *Cell* **1997**, *89*, 1175.
(72) Ferreon, J. C.; Lee, C. W.; Arai, M.; Martinez-Yamout, M. A.; Dyson, H. J.; Wright, P. E. *Proc. Natl. Acad. Sci. U.S.A.* **2009**, *106*, 6591.
(73) Teufel, D. P.; Freund, S. M.; Bycroft, M.; Fersht, A. R. *Proc. Natl. Acad. Sci. U.S.A.* **2007**, *104*, 7009.
(74) Padmanabhan, S.; Baldwin, R. L. *Protein Sci.* **1994**, *3*, 1992.
(75) Padmanabhan, S.; Baldwin, R. L. *J. Mol. Biol.* **1994**, *241*, 706.
(76) Luo, P.; Baldwin, R. L. *Biophys. Chem.* **2002**, *96*, 103.
(77) Munoz, V.; Serrano, L. *Nat. Struct. Biol.* **1994**, *1*, 399.
(78) Creamer, T. P.; Rose, G. D. *Protein Sci.* **1995**, *4*, 1305.
(79) Kutchukian, P. S.; Yang, J. S.; Verdine, G. L.; Shakhnovich, E. I. *J. Am. Chem. Soc.* **2009**, *131*, 4622.
(80) Bautista, A. D.; Appelbaum, J. S.; Craig, C. J.; Michel, J.; Schepartz, A. *J. Am. Chem. Soc.* **2010**, *132*, 2904.
(81) Kim, Y. W.; Kutchukian, P. S.; Verdine, G. L. *Org. Lett.* **2010**, *12*, 3046.
(82) Shoemaker, B. A.; Portman, J. J.; Wolynes, P. G. *Proc. Natl. Acad. Sci. U.S.A.* **2000**, *97*, 8868.